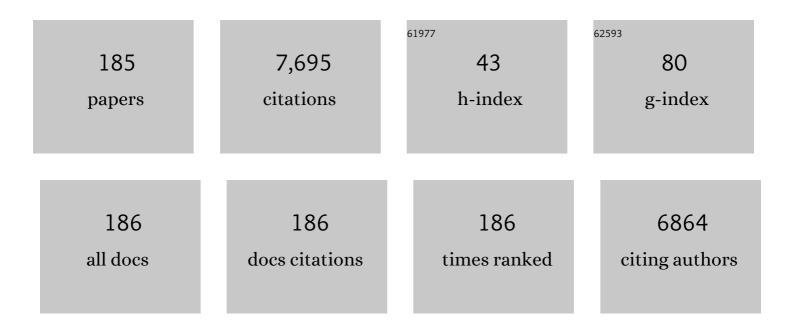
## Do Heui Kim

List of Publications by Year in descending order

Source: https://exaly.com/author-pdf/9033937/publications.pdf Version: 2024-02-01



Do Helli Kim

#	Article	IF	CITATIONS
1	Upgrading bio-oil model compound over bifunctional Ru/HZSM-5 catalysts in biphasic system: Complete hydrodeoxygenation of vanillin. Journal of Hazardous Materials, 2022, 423, 126525.	12.4	24
2	Enhanced SO2 resistance of V2O5/WO3-TiO2 catalyst physically mixed with alumina for the selective catalytic reduction of NOx with NH3. Chemical Engineering Journal, 2022, 433, 133836.	12.7	19
3	Top-down HCl treatment to prepare highly active Ga species in Ga/ZSM-5 for propane aromatization. Fuel Processing Technology, 2022, 227, 107107.	7.2	8
4	Alleviating inhibitory effect of H2 on low-temperature water-gas shift reaction activity of Pt/CeO2 catalyst by forming CeO2 nano-patches on Pt nano-particles. Applied Catalysis B: Environmental, 2022, 305, 121038.	20.2	11
5	Aggregation of CeO <sub>2</sub> particles with aligned grains drives sintering of Pt single atoms in Pt/CeO <sub>2</sub> catalysts. Journal of Materials Chemistry A, 2022, 10, 7029-7035.	10.3	2
6	Enhancement in the metal efficiency of Ru/TiO2 catalyst for guaiacol hydrogenation via hydrogen spillover in the liquid phase. Journal of Catalysis, 2022, 410, 93-102.	6.2	13
7	<i>In situ</i> spectroscopic studies of the effect of water on the redox cycle of Cu ions in Cu-SSZ-13 during selective catalytic reduction of NO <sub><i>x</i></sub> . Chemical Communications, 2022, 58, 6610-6613.	4.1	12
8	System-Level Analysis of Methanol Production from Shale Gas Integrated with Multibed-BTX Production. ACS Sustainable Chemistry and Engineering, 2022, 10, 5998-6011.	6.7	10
9	Tailoring the mechanochemical interaction between vanadium oxides and zeolite for sulfur-resistant DeNO catalysts. Applied Catalysis B: Environmental, 2022, 316, 121672.	20.2	9
10	Deactivation resistance effect of alkane co-feeding on methane dehydroaromatization and active GaO+ species in Ga/HZSM-5 for BTX production. Fuel, 2022, 325, 124939.	6.4	6
11	System-level analysis for continuous BTX production from shale gas over Mo/HZSM-5 catalyst: Promotion effects of CO2 co-feeding on process economics and environment. Chemical Engineering Journal, 2022, 450, 137992.	12.7	10
12	Improving the efficiency of Ru metal supported on SiO2 in liquid-phase hydrogenation of gluconic acid by adding activated carbon. Chemical Engineering Journal, 2022, 450, 138149.	12.7	9
13	Deactivation of Pd/Zeolites passive NOx adsorber induced by NO and H2O: Comparative study of Pd/ZSM-5 and Pd/SSZ-13. Catalysis Today, 2021, 360, 350-355.	4.4	21
14	Improved catalytic performance and resistance to SO2 over V2O5-WO3/TiO2 catalyst physically mixed with Fe2O3 for low-temperature NH3-SCR. Catalysis Today, 2021, 376, 95-103.	4.4	37
15	Uniform synthesis of palladium species confined in a small-pore zeolite <i>via</i> full ion-exchange investigated by cryogenic electron microscopy. Journal of Materials Chemistry A, 2021, 9, 19796-19806.	10.3	15
16	Control of the Cu ion species in Cu-SSZ-13 <i>via</i> the introduction of Co <sup>2+</sup> co-cations to improve the NH <sub>3</sub> -SCR activity. Catalysis Science and Technology, 2021, 11, 4838-4848.	4.1	11
17	Simple physical mixing of zeolite prevents sulfur deactivation of vanadia catalysts for NOx removal. Nature Communications, 2021, 12, 901.	12.8	49
18	Pt nanoparticles encapsulated in CeO2 over-layers synthesized by controlled reductive treatment to suppress CH4 formation in high-temperature water-gas shift reaction. Journal of Catalysis, 2021, 395, 246-257.	6.2	12

#	Article	IF	CITATIONS
19	Mobility of Cu Ions in Cu-SSZ-13 Determines the Reactivity of Selective Catalytic Reduction of NO <sub><i>x</i></sub> with NH <sub>3</sub> . Journal of Physical Chemistry Letters, 2021, 12, 3210-3216.	4.6	33
20	Effects of Ce/Al molar ratio in Ce-incorporated mesoporous SAPO-34 on the physicochemical property and catalytic performance in the selective production of light olefins via conversion of chloromethane. Applied Catalysis A: General, 2021, 615, 118061.	4.3	1
21	Promoting the Methane Oxidation on Pd/CeO <sub>2</sub> Catalyst by Increasing the Surface Oxygen Mobility via Defect Engineering. ChemCatChem, 2021, 13, 3706-3712.	3.7	8
22	Enhanced activity of vanadia supported on microporous titania for the selective catalytic reduction of NO with NH3: Effect of promoters. Chemosphere, 2021, 275, 130105.	8.2	7
23	Evaluation of Pd/ZSM-5 catalyst for simultaneous reaction of transesterification and partial catalytic transfer hydrogenation of soybean oil under supercritical methanol. Fuel Processing Technology, 2021, 218, 106870.	7.2	14
24	Methane combustion over mesoporous cobalt oxide catalysts: Effects of acid treatment. Molecular Catalysis, 2021, 511, 111728.	2.0	7
25	Synthesis of aluminum and gallium-incorporated MFI zeotypes and their catalytic activity for ethane dehydroaromatization. Microporous and Mesoporous Materials, 2021, 323, 111243.	4.4	5
26	Highly selective production of syngas (>99%) in the partial oxidation of methane at 480°C over Pd/CeO2 catalyst promoted by HCl. Applied Surface Science, 2021, 560, 150043.	6.1	6
27	Coaromatization of methane and propane over Ga supported on HZSM-5 catalysts: The effect of mesoporosity on deactivation behavior. Fuel, 2021, 304, 121497.	6.4	5
28	Enhanced reactivity and stability in methane dehydro-aromatization over Mo/HZSM-5 physically mixed with NiO. Applied Catalysis B: Environmental, 2021, 296, 120377.	20.2	20
29	Ag-doped manganese oxide catalyst for gasoline particulate filters: Effect of crystal phase on soot oxidation activity. Applied Surface Science, 2021, 569, 151041.	6.1	15
30	Catalytic hydrogenation of alginic acid into sugar alcohols over ruthenium supported on nitrogen-doped mesoporous carbons. Catalysis Today, 2020, 352, 66-72.	4.4	12
31	Selective catalytic reduction of NO by ammonia and NO oxidation Over CoOx/CeO2 catalysts. Molecular Catalysis, 2020, 482, 110664.	2.0	9
32	NO reduction by CO over CoOx/CeO2 catalysts: Effect of support calcination temperature on activity. Molecular Catalysis, 2020, 482, 110703.	2.0	10
33	Oxidative Methane Conversion to Ethane on Highly Oxidized Pd/CeO <sub>2</sub> Catalysts Below 400 °C. ChemSusChem, 2020, 13, 677-681.	6.8	16
34	Controlling Catalytic Selectivity Mediated by Stabilization of Reactive Intermediates in Small-Pore Environments: A Study of Mn/TiO <sub>2</sub> in the NH <sub>3</sub> -SCR Reaction. ACS Catalysis, 2020, 10, 12017-12030.	11.2	40
35	Kinetic and DRIFTS studies of IrRu/Al <sub>2</sub> O <sub>3</sub> catalysts for lean NO <sub>x</sub> reduction by CO at low temperature. Catalysis Science and Technology, 2020, 10, 8182-8195.	4.1	11
36	Time-resolved observation of V <sub>2</sub> O <sub>5</sub> /TiO <sub>2</sub> in NH <sub>3</sub> -SCR reveals the equivalence of BrÃ,nsted and Lewis acid sites. Chemical Communications, 2020, 56, 15450-15453.	4.1	22

#	Article	IF	CITATIONS
37	Hydrogenolysis of alginic acid over mono and bimetallic ruthenium/nickel supported on activated carbon catalysts with basic promoters. Reaction Chemistry and Engineering, 2020, 5, 1783-1790.	3.7	1
38	Effects of Co/Al molar ratio in CoAPSO-34 catalysts on the physicochemical property and catalytic performance in the chloromethane to light olefins reaction. Applied Catalysis A: General, 2020, 603, 117762.	4.3	5
39	Hydrogen production from formic acid dehydrogenation over a Pd supported on N-doped mesoporous carbon catalyst: A role of nitrogen dopant. Applied Catalysis A: General, 2020, 608, 117887.	4.3	31
40	Recent advances in catalytic co-pyrolysis of biomass and plastic waste for the production of petroleum-like hydrocarbons. Bioresource Technology, 2020, 310, 123473.	9.6	199
41	Improving NOx storage and CO oxidation abilities of Pd/SSZ-13 by increasing its hydrophobicity. Applied Catalysis B: Environmental, 2020, 277, 119190.	20.2	43
42	One-pot conversion of alginic acid into furfural using Amberlyst-15 as a solid acid catalyst in γ-butyrolactone/water co-solvent system. Environmental Research, 2020, 187, 109667.	7.5	25
43	Hydrogen production by the steam reforming of ethanol over K-promoted Co/Al2O3–CaO xerogel catalysts. Molecular Catalysis, 2020, 491, 110980.	2.0	18
44	Effects of Ni loading on the physicochemical properties of NiO <sub>x</sub> /CeO <sub>2</sub> catalysts and catalytic activity for NO reduction by CO. Catalysis Science and Technology, 2020, 10, 2359-2368.	4.1	20
45	Mechanistic insights on aqueous formic acid dehydrogenation over Pd/C catalyst for efficient hydrogen production. Journal of Catalysis, 2020, 389, 506-516.	6.2	48
46	Lean NO <sub>x</sub> reduction by CO at low temperature over bimetallic IrRu/Al <sub>2</sub> O <sub>3</sub> catalysts with different Ir : Ru ratios. Catalysis Science and Technology, 2020, 10, 2120-2136.	4.1	22
47	Preparation of HZSM-5 catalysts with different ratios of structure directing agents and their effects on the decomposition of exo-tetrahydrodicyclopentadiene under supercritical conditions and coke formation. Applied Surface Science, 2020, 511, 145398.	6.1	8
48	Understanding the dynamic behavior of acid sites on TiO2-supported vanadia catalysts via operando DRIFTS under SCR-relevant conditions. Journal of Catalysis, 2020, 382, 269-279.	6.2	53
49	Promotional effect of Au on Fe/HZSM-5 catalyst for methane dehydroaromatization. Fuel, 2020, 274, 117852.	6.4	16
50	NOx Reduction by CO over Ir-based Bimetallic Catalysts. Transactions of the Korean Society of Automotive Engineers, 2020, 28, 359-365.	0.3	1
51	Comparative study of the mobility of Pd species in SSZ-13 and ZSM-5, and its implication for their activity as passive NO <sub>x</sub> adsorbers (PNAs) after hydro-thermal aging. Catalysis Science and Technology, 2019, 9, 163-173.	4.1	58
52	Effect of Reactant Ratios on Methane Oxychlorination Over CeO <sub>2</sub> Catalyst. Journal of Nanoscience and Nanotechnology, 2019, 19, 5961-5964.	0.9	0
53	Comparison of NOx Adsorption/Desorption Behaviors over Pd/CeO2 and Pd/SSZ-13 as Passive NOx Adsorbers for Cold Start Application. Emission Control Science and Technology, 2019, 5, 172-182.	1.5	28
54	Enhanced yield of benzene, toulene, and xylene from the co-aromatization of methane and propane over gallium supported on mesoporous ZSM-5 and ZSM-11. Fuel, 2019, 251, 404-412.	6.4	33

#	Article	IF	CITATIONS
55	Effects of Molecular and Electronic Structures in CoO <i><sub>x</sub></i> /CeO <sub>2</sub> Catalysts on NO Reduction by CO. Journal of Physical Chemistry C, 2019, 123, 7166-7177.	3.1	29
56	Characteristics of Mn/H-ZSM-5 catalysts for methane dehydroaromatization. Applied Catalysis A: General, 2019, 577, 10-19.	4.3	15
57	Sulfur resistance of Ca-substituted LaCoO3 catalysts in CO oxidation. Molecular Catalysis, 2019, 468, 148-153.	2.0	21
58	Effect of Cu addition to carbon-supported Ru catalysts on hydrogenation of alginic acid into sugar alcohols. Applied Catalysis A: General, 2019, 578, 98-104.	4.3	14
59	Catalytic Cleavage of Ether Bond in a Lignin Model Compound over Carbon-Supported Noble Metal Catalysts in Supercritical Ethanol. Catalysts, 2019, 9, 158.	3.5	7
60	Oxidation of C3H8, iso-C5H12 and C3H6 under near-stoichiometric and fuel-lean conditions over aged Pt–Pd/Al2O3 catalysts with different Pt:Pd ratios. Applied Catalysis B: Environmental, 2019, 251, 283-294.	20.2	29
61	Inter-particle migration of Cu ions in physically mixed Cu-SSZ-13 and H-SSZ-13 treated by hydrothermal aging. Reaction Chemistry and Engineering, 2019, 4, 1059-1066.	3.7	22
62	Propylene epoxidation by oxygen over tungsten oxide supported on ceria-zirconia. Molecular Catalysis, 2019, 467, 111-119.	2.0	5
63	Effect of the Si/Al ratio in Ga/mesoporous HZSM-5 on the production of benzene, toluene, and xylene <i>via</i> coaromatization of methane and propane. Catalysis Science and Technology, 2019, 9, 6285-6296.	4.1	15
64	Hydrothermal Synthesis of Titanate Nanotubes with Different Pore Structure and its Effect on the Catalytic Performance of V2O5-WO3/Titanate Nanotube Catalysts for NH3-SCR. Topics in Catalysis, 2019, 62, 214-218.	2.8	4
65	Effect of reduction treatments (H2 vs. CO) on the NO adsorption ability and the physicochemical properties of Pd/SSZ-13 passive NOx adsorber for cold start application. Applied Catalysis A: General, 2019, 569, 28-34.	4.3	61
66	Understanding the effect of Pd size on formic acid dehydrogenation via size-controlled Pd/C catalysts prepared by NaBH4 treatment. Applied Catalysis B: Environmental, 2019, 244, 684-693.	20.2	108
67	Effect of various activation conditions on the low temperature NO adsorption performance of Pd/SSZ-13 passive NOx adsorber. Catalysis Today, 2019, 320, 175-180.	4.4	81
68	Ag-(Mo-W)/ZrO2 catalysts for the production of propylene oxide: Effect of pH in the preparation of ZrO2 support. Catalysis Communications, 2018, 111, 80-83.	3.3	14
69	Influence of the Defect Concentration of Ceria on the Pt Dispersion and the CO Oxidation Activity of Pt/CeO <sub>2</sub> . Journal of Physical Chemistry C, 2018, 122, 4972-4983.	3.1	62
70	Investigation on the enhanced catalytic activity of a Ni-promoted Pd/C catalyst for formic acid dehydrogenation: effects of preparation methods and Ni/Pd ratios. RSC Advances, 2018, 8, 2441-2448.	3.6	27
71	Effect of Si/Al 2 ratios in Mo/H-MCM-22 on methane dehydroaromatization. Applied Catalysis A: General, 2018, 552, 11-20.	4.3	31
72	Plasma assisted oxidative coupling of methane (OCM) over Ag/SiO2 and subsequent regeneration at low temperature. Applied Catalysis A: General, 2018, 557, 39-45.	4.3	16

#	Article	IF	CITATIONS
73	In Situ Elucidation of the Active State of Co–CeO <sub><i>x</i></sub> Catalysts in the Dry Reforming of Methane: The Important Role of the Reducible Oxide Support and Interactions with Cobalt. ACS Catalysis, 2018, 8, 3550-3560.	11.2	80
74	Low temperature NO adsorption over hydrothermally aged Pd/CeO2 for cold start application. Catalysis Today, 2018, 307, 93-101.	4.4	55
75	Effect of pore structure of TiO 2 on the SO 2 poisoning over V 2 O 5 /TiO 2 catalysts for selective catalytic reduction of NO x with NH 3. Catalysis Today, 2018, 303, 19-24.	4.4	39
76	Suppressed Strong Metal–Support Interactions in Platinum on Sulfated Titania and Their Influence on the Oxidation of Carbon Monoxide. ChemCatChem, 2018, 10, 1258-1262.	3.7	11
77	Investigation of the active sites and optimum Pd/Al of Pd/ZSM–5 passive NO adsorbers for the cold-start application: Evidence of isolated-Pd species obtained after a high-temperature thermal treatment. Applied Catalysis B: Environmental, 2018, 226, 71-82.	20.2	89
78	Rotation-Assisted Hydrothermal Synthesis of Thermally Stable Multiwalled Titanate Nanotubes and Their Application to Selective Catalytic Reduction of NO with NH <sub>3</sub> . ACS Applied Materials & Interfaces, 2018, 10, 42249-42257.	8.0	14
79	Oxychlorination of methane over FeOx/CeO2 catalysts. Korean Journal of Chemical Engineering, 2018, 35, 2185-2190.	2.7	10
80	Direct methanol synthesis from methane in a plasma-catalyst hybrid system at low temperature using metal oxide-coated glass beads. Scientific Reports, 2018, 8, 9956.	3.3	13
81	Chemisorption of NH <sub>3</sub> on Monomeric Vanadium Oxide Supported on Anatase TiO <sub>2</sub> : A Combined DRIFT and DFT Study. Journal of Physical Chemistry C, 2018, 122, 16674-16682.	3.1	36
82	Synthesis of faulted CHA-type zeolites with controllable faulting probability. Microporous and Mesoporous Materials, 2018, 256, 266-274.	4.4	8
83	Effect of Soot on N2O Formation Over Pt Based Diesel Oxidation Catalyst Supported on Microporous TiO2. Topics in Catalysis, 2017, 60, 361-366.	2.8	2
84	Effect of niobium oxide phase on the furfuryl alcohol dehydration. Catalysis Communications, 2017, 97, 65-69.	3.3	42
85	Activation of Pd/SSZ-13 catalyst by hydrothermal aging treatment in passive NO adsorption performance at low temperature for cold start application. Applied Catalysis B: Environmental, 2017, 212, 140-149.	20.2	127
86	Effects of microporous TiO 2 support on the catalytic and structural properties of V 2 O 5 /microporous TiO 2 for the selective catalytic reduction of NO by NH 3. Applied Catalysis B: Environmental, 2017, 210, 421-431.	20.2	78
87	Depolymerization of Protobind lignin to produce monoaromatic compounds over Cu/ZSM-5 catalyst in supercritical ethanol. Molecular Catalysis, 2017, 442, 140-146.	2.0	26
88	Catalytic Hydrogenation of Macroalgaeâ€Đerived Alginic Acid into Sugar Alcohols. ChemSusChem, 2017, 10, 4891-4898.	6.8	9
89	BTX production by coaromatization of methane and propane over gallium oxide supported on mesoporous HZSM-5. Molecular Catalysis, 2017, 439, 134-142.	2.0	21
90	Effect of sulfur aging and regeneration on low temperature NO adsorption over hydrothermally treated Pd/CeO 2 and Pd/Ce 0.58 Zr 0.42 O 2 catalysts. Catalysis Today, 2017, 297, 53-59.	4.4	35

#	Article	IF	CITATIONS
91	Facile Synthesis of KFI-type Zeolite and Its Application to Selective Catalytic Reduction of NO <sub><i>x</i></sub> with NH <sub>3</sub> . ACS Catalysis, 2017, 7, 6070-6081.	11.2	83
92	Decomposition of Lignin Using MO–MgAlOy Mixed Oxide Catalysts (M=Co, Ni and Cu) in Supercritical Ethanol. Topics in Catalysis, 2017, 60, 637-643.	2.8	2
93	Hydrothermal Conversion of Alginate into Uronic Acids over a Sulfonated Glucoseâ€Derived Carbon Catalyst. ChemCatChem, 2017, 9, 329-337.	3.7	9
94	Ordered mesoporous MCo2O4 (M = Cu, Zn and Ni) spinel catalysts with high catalytic performance for methane combustion. Journal of Molecular Catalysis A, 2017, 426, 68-74.	4.8	44
95	Synthesis of terraced and spherical MgO nanoparticles using flame metal combustion. Powder Technology, 2017, 305, 132-140.	4.2	20
96	Benzene, Toluene, and Xylene Production by Direct Dehydroaromatization of Methane Over WOy/HZSM-5 Catalysts. Journal of Nanoscience and Nanotechnology, 2017, 17, 8226-8231.	0.9	2
97	Lignin Depolymerization Over CuO–MgO–Al <sub>2</sub> O <sub>3</sub> Mixed Oxide Catalysts in Supercritical Ethanol: Effect of Catalyst Preparation Methods. Nanoscience and Nanotechnology Letters, 2017, 9, 161-164.	0.4	1
98	Direct catalytic conversion of brown seaweed-derived alginic acid to furfural using 12-tungstophosphoric acid catalyst in tetrahydrofuran/water co-solvent. Energy Conversion and Management, 2016, 118, 135-141.	9.2	24
99	Catalytic Conversion of Macroalgae-derived Alginate to Useful Chemicals. Catalysis Surveys From Asia, 2016, 20, 195-209.	2.6	9
100	Synthesis of Dimethyl Carbonate from Propylene Carbonate and Methanol Over Y <sub>2</sub> 0 <sub>3</sub> /CeO <sub>2</sub> –La <sub>2Catalysts. Journal of Nanoscience and Nanotechnology, 2016, 16, 10810-10815.</sub>	UB>O8	lt; <b>S</b> UB>38،
101	Production of furfural from macroalgae-derived alginic acid over Amberlyst-15. Journal of Molecular Catalysis A, 2016, 423, 264-269.	4.8	22
102	Hydrogen production by steam reforming of ethanol over Ni-Sr-Al 2 O 3 -ZrO 2 aerogel catalyst. Journal of Molecular Catalysis A, 2016, 424, 342-350.	4.8	16
103	How Pt Interacts with CeO <sub>2</sub> under the Reducing and Oxidizing Environments at Elevated Temperature: The Origin of Improved Thermal Stability of Pt/CeO <sub>2</sub> Compared to CeO <sub>2</sub> . Journal of Physical Chemistry C, 2016, 120, 25870-25879.	3.1	185
104	Sulfation and Desulfation Behavior of Pt–BaO/MgO–Al <sub>2</sub> O <sub>3</sub> NOx Storage Reduction Catalyst. Journal of Nanoscience and Nanotechnology, 2016, 16, 4411-4416.	0.9	1
105	Characteristics of Manganese Supported on Hydrous Titanium Oxide Catalysts for the Selective Catalytic Reduction of NOx with Ammonia. Topics in Catalysis, 2016, 59, 1008-1012.	2.8	12
106	Roles of Promoters in V <sub>2</sub> O <sub>5</sub> /TiO <sub>2</sub> Catalysts for Selective Catalytic Reduction of NOx with NH <sub>3</sub> : Effect of Order of Impregnation. Journal of Nanoscience and Nanotechnology, 2016, 16, 4350-4356.	0.9	14
107	CeO2-TiO2 catalyst prepared by physical mixing for NH3 selective catalytic reduction: Evidence about the migration of sulfates from TiO2 to CeO2 via simple calcination. Korean Journal of Chemical Engineering, 2016, 33, 2547-2554.	2.7	14
108	Hydrothermal conversion of alginic acid to furfural catalyzed by Cu(II) ion. Catalysis Today, 2016, 265, 154-162.	4.4	18

#	Article	IF	CITATIONS
109	Catalytic Copyrolysis of Cellulose and Thermoplastics over HZSM-5 and HY. ACS Sustainable Chemistry and Engineering, 2016, 4, 1354-1363.	6.7	113
110	Hydrogen production by steam reforming of ethanol over Ni–X/Al 2 O 3 –ZrO 2 (X = Mg, Ca, Sr, and Ba) xerogel catalysts: Effect of alkaline earth metal addition. Journal of Molecular Catalysis A, 2016, 415, 151-159.	4.8	35
111	Hydrothermal conversion of macroalgae-derived alginate to lactic acid catalyzed by metal oxides. Catalysis Science and Technology, 2016, 6, 1146-1156.	4.1	23
112	Suppressed N2O formation during NH3 selective catalytic reduction using vanadium on zeolitic microporous TiO2. Scientific Reports, 2015, 5, 12702.	3.3	24
113	Complementary effect of plasma–catalysis hybrid system on methane complete oxidation over non-PGM catalysts. Catalysis Communications, 2015, 69, 223-227.	3.3	7
114	2â€Butanol Dehydration over Highly Dispersed Molybdenum Oxide/ <scp>MCM</scp> â€41 Catalysts. Bulletin of the Korean Chemical Society, 2015, 36, 1974-1979.	1.9	0
115	Promotional Effect on Selective Catalytic Reduction of NO <sub><i>x</i></sub> with NH <sub>3</sub> over Overloaded W and Ce on V <sub>2</sub> O <sub>5</sub> /TiO <sub>2</sub> Catalysts. Journal of Nanomaterials, 2015, 2015, 1-7.	2.7	8
116	Catalytic hydrodeoxygenation of 2-methoxy phenol and dibenzofuran over Pt/mesoporous zeolites. Energy, 2015, 81, 33-40.	8.8	83
117	Catalytic hydrothermal conversion of macroalgae-derived alginate: effect of pH on production of furfural and valuable organic acids under subcritical water conditions. Journal of Molecular Catalysis A, 2015, 399, 106-113.	4.8	31
118	Effect of Co/Ni ratios in cobalt nickel mixed oxide catalysts on methane combustion. Applied Catalysis A: General, 2015, 505, 62-69.	4.3	89
119	Roles of ZrO2 in SO2-poisoned Pd/(Ce-Zr)O2 catalysts for CO oxidation. Catalysis Today, 2015, 258, 518-524.	4.4	28
120	Effect of surfactant, HCl and NH3 treatments on the regeneration of waste activated carbon used in selective catalytic reduction unit. Journal of Industrial and Engineering Chemistry, 2015, 32, 109-112.	5.8	20
121	Synergistic effect of non-thermal plasma–catalysis hybrid system on methane complete oxidation over Pd-based catalysts. Chemical Engineering Journal, 2015, 259, 761-770.	12.7	72
122	Removal of NOx at Low Temperature Over Mesoporous <i>α</i> -Mn <sub>2</sub> O <sub>3</sub> Catalyst. Journal of Nanoscience and Nanotechnology, 2014, 14, 2527-2531.	0.9	9
123	Effect of Mg/Al ratios on the NOx storage activity over Pt-BaO/Mg–Al mixed oxides. Catalysis Today, 2014, 231, 155-163.	4.4	14
124	Effect of oxidation states of vanadium precursor solution in V2O5/TiO2 catalysts for low temperature NH3 selective catalytic reduction. Catalysis Today, 2014, 232, 185-191.	4.4	55
125	Sulfation and Desulfation Mechanisms on Pt–BaO/Al2O3 NOx Storage-Reduction (NSR) Catalysts. Catalysis Surveys From Asia, 2014, 18, 13-23.	2.6	5
126	Effect of H <sub>2</sub> O on the Morphological Changes of KNO <sub>3</sub> Formed on K <sub>2</sub> O/Al <sub>2</sub> O <sub>3</sub> NO <sub><i>x</i></sub> Storage Materials: Fourier Transform Infrared and Time-Resolved X-ray Diffraction Studies. Journal of Physical Chemistry C, 2014, 118, 4189-4197.	3.1	14

#	Article	IF	CITATIONS
127	Effects of potassium loading and thermal aging on K/Pt/Al2O3 high-temperature lean NOx trap catalysts. Catalysis Today, 2014, 231, 164-172.	4.4	21
128	Catalytic Characteristics of Titanium Oxide/MCM-41 Synthesized by Liquid Phase Atomic Layer Deposition. Journal of Nanoscience and Nanotechnology, 2013, 13, 1988-1992.	0.9	3
129	Butanol Dehydration over V2O5-TiO2/MCM-41 Catalysts Prepared via Liquid Phase Atomic Layer Deposition. Materials, 2013, 6, 1718-1729.	2.9	13
130	Effect of sulfur loading on the desulfation chemistry of a commercial lean NOx trap catalyst. Catalysis Today, 2012, 197, 3-8.	4.4	11
131	Preparation of Highly Dispersed Tungsten Oxide on MCM-41 via Atomic Layer Deposition and Its Application to Butanol Dehydration. Journal of Nanoscience and Nanotechnology, 2012, 12, 6074-6079.	0.9	7
132	Enhanced High Temperature Performance of MgAl2O4-Supported Pt–BaO Lean NOx Trap Catalysts. Topics in Catalysis, 2012, 55, 70-77.	2.8	12
133	Synthesis of butenes through 2-butanol dehydration over mesoporous materials produced from ferrierite. Catalysis Today, 2012, 185, 191-197.	4.4	25
134	Thermal durability of Cu-CHA NH3-SCR catalysts for diesel NO reduction. Catalysis Today, 2012, 184, 252-261.	4.4	245
135	Possible origin of improved high temperature performance of hydrothermally aged Cu/beta zeolite catalysts. Catalysis Today, 2012, 184, 245-251.	4.4	35
136	Deactivation mechanisms of Pt/Pd-based diesel oxidation catalysts. Catalysis Today, 2012, 184, 197-204.	4.4	86
137	Characteristics of Pt–K/MgAl2O4 lean NOx trap catalysts. Catalysis Today, 2012, 184, 2-7.	4.4	27
138	Effects of La <sub>2</sub> O <sub>3</sub> on the Mixed Higher Alcohols Synthesis from Syngas over Co Catalysts: A Combined Theoretical and Experimental Study. Journal of Physical Chemistry C, 2011, 115, 17440-17451.	3.1	119
139	Utilization of a By-Product Produced from Oxidative Desulfurization Process Over Cs-Mesoporous Silica Catalysts. Journal of Nanoscience and Nanotechnology, 2011, 11, 1706-1709.	0.9	4
140	Effect of reductive treatments on Pt behavior and NOx storage in lean NOx trap catalysts. Catalysis Today, 2011, 175, 78-82.	4.4	4
141	Octene hydroformylation by using rhodium complexes tethered onto selectively functionalized mesoporous silica and in situ high pressure IR study. Catalysis Today, 2011, 164, 561-565.	4.4	7
142	Water-induced formation of cobalt oxides over supported cobalt/ceria–zirconia catalysts under ethanol-steam conditions. Journal of Catalysis, 2010, 273, 229-235.	6.2	77
143	Excellent activity and selectivity of Cu-SSZ-13 in the selective catalytic reduction of NOx with NH3. Journal of Catalysis, 2010, 275, 187-190.	6.2	674
144	The different impacts of SO2 and SO3 on Cu/zeolite SCR catalysts. Catalysis Today, 2010, 151, 266-270.	4.4	96

#	Article	IF	CITATIONS
145	Coordinatively Unsaturated Al <sup>3+</sup> Centers as Binding Sites for Active Catalyst Phases of Platinum on γ-Al <sub>2</sub> O <sub>3</sub> . Science, 2009, 325, 1670-1673.	12.6	790
146	Understanding the nature of surface nitrates in BaO/ $\hat{I}^3$ -Al2O3 NOx storage materials: A combined experimental and theoretical study. Journal of Catalysis, 2009, 261, 17-22.	6.2	79
147	Promotional Effect of CO2 on Desulfation Processes for Pre-Sulfated Pt-BaO/Al2O3 Lean NOx Trap Catalysts. Topics in Catalysis, 2009, 52, 1719-1722.	2.8	3
148	Metallic phases of cobalt-based catalysts in ethanol steam reforming: The effect of cerium oxide. Applied Catalysis A: General, 2009, 355, 69-77.	4.3	99
149	Effects of Sulfation Level on the Desulfation Behavior of Presulfated Pt-BaO/Al <sub>2</sub> O <sub>3</sub> Lean NO <i><sub>x</sub></i> Trap Catalysts: A Combined H <sub>2</sub> Temperature-Programmed Reaction, in Situ Sulfur K-Edge X-ray Absorption Near-Edge Spectroscopy, X-ray Photoelectron Spectroscopy, and Time-Resolved X-ray Diffraction Study. Journal	3.1	17
150	of Physical Chemistry C, 2009, 113, 7336-7341. Characteristics of Desulfation Behavior for Presulfated Pt-BaO/CeO2 Lean NOx Trap Catalyst: The Role of the CeO2 Support. Journal of Physical Chemistry C, 2009, 113, 21123-21129.	3.1	14
151	Characterization of surface and bulk nitrates of γ-Al2O3–supported alkaline earth oxides using density functional theory. Physical Chemistry Chemical Physics, 2009, 11, 3380.	2.8	10
152	Hydrogen Production from Ethanol Steam Reforming Over Supported Cobalt Catalysts. Catalysis Letters, 2008, 122, 295-301.	2.6	61
153	Promotional Effects of H2O Treatment on NO x Storage Over Fresh and Thermally Aged Pt–BaO/Al2O3 Lean NO x Trap Catalysts. Catalysis Letters, 2008, 124, 39-45.	2.6	13
154	Sequential high temperature reduction, low temperature hydrolysis for the regeneration of sulfated NOx trap catalysts. Catalysis Today, 2008, 136, 183-187.	4.4	10
155	NOx uptake on alkaline earth oxides (BaO, MgO, CaO and SrO) supported on Î <sup>3</sup> -Al2O3. Catalysis Today, 2008, 136, 121-127.	4.4	27
156	Excellent sulfur resistance of Pt/BaO/CeO2 lean NOx trap catalysts. Applied Catalysis B: Environmental, 2008, 84, 545-551.	20.2	55
157	Role of Pentacoordinated Al <sup>3+</sup> Ions in the High Temperature Phase Transformation of γ-Al <sub>2</sub> O <sub>3</sub> . Journal of Physical Chemistry C, 2008, 112, 9486-9492.	3.1	106
158	Roles of Pt and BaO in the Sulfation of Pt/BaO/Al <sub>2</sub> O <sub>3</sub> Lean NO <i><sub>x</sub></i> Trap Materials:  Sulfur K-edge XANES and Pt L <sub>III</sub> XAFS Studies. Journal of Physical Chemistry C, 2008, 112, 2981-2987.	3.1	17
159	Adsorption and Formation of BaO Overlayers on γ-Al <sub>2</sub> O <sub>3</sub> Surfaces. Journal of Physical Chemistry C, 2008, 112, 18050-18060.	3.1	29
160	Synthesis of nanoporous zirconium oxophosphate and application for removal of U(VI). Water Research, 2007, 41, 3217-3226.	11.3	45
161	Design of a Reaction Protocol for Decoupling Sulfur Removal and Thermal Aging Effects during Desulfation of Ptâ^'BaO/Al2O3 Lean NOx Trap Catalysts. Industrial & Engineering Chemistry Research, 2007, 46, 2735-2740.	3.7	11
162	Water-Induced Morphology Changes in BaO/γ-Al2O3NOxStorage Materials:  an FTIR, TPD, and Time-Resolved Synchrotron XRD Study. Journal of Physical Chemistry C, 2007, 111, 4678-4687.	3.1	35

#	Article	IF	CITATIONS
163	HRTEM Study of diesel soot collected from diesel particulate filters. Carbon, 2007, 45, 70-77.	10.3	239
164	Penta-coordinated Al3+ ions as preferential nucleation sites for BaO on γ-Al2O3: An ultra-high-magnetic field 27Al MAS NMR study. Journal of Catalysis, 2007, 251, 189-194.	6.2	173
165	Water-induced bulk Ba(NO3)2 formation from NO2 exposed thermally aged BaO/Al2O3. Applied Catalysis B: Environmental, 2007, 72, 233-239.	20.2	39
166	Effect of Barium Loading on the Desulfation of Pt-BaO/Al2O3Studied by H2TPRX, TEM, Sulfur K-edge XANES, and in Situ TR-XRD. Journal of Physical Chemistry B, 2006, 110, 10441-10448.	2.6	30
167	Relationship of Pt Particle Size to the NOxStorage Performance of Thermally Aged Pt/BaO/Al2O3Lean NOxTrap Catalysts. Industrial & Engineering Chemistry Research, 2006, 45, 8815-8821.	3.7	51
168	Effects of Ba loading and calcination temperature on BaAl2O4 formation for BaO/Al2O3 NOx storage and reduction catalysts. Catalysis Today, 2006, 114, 86-93.	4.4	70
169	NO x uptake mechanism on Pt/BaO/Al2O3 catalysts. Catalysis Letters, 2006, 111, 119-126.	2.6	46
170	Differential kinetic analysis of diesel particulate matter (soot) oxidation by oxygen using a step–response technique. Applied Catalysis B: Environmental, 2005, 61, 120-129.	20.2	119
171	Changes in Ba Phases in BaO/Al2O3 upon Thermal Aging and H2O Treatment. Catalysis Letters, 2005, 105, 259-268.	2.6	43
172	NO2Adsorption on BaO/Al2O3:Â The Nature of Nitrate Species. Journal of Physical Chemistry B, 2005, 109, 27-29.	2.6	117
173	Comparison of Two Preparation Methods in the Redox Properties of Pd/CeO2/Ta/Si Model Catalysts: Spin Coating Versus Sputter Deposition. Catalysis Letters, 2004, 98, 23-28.	2.6	8
174	Effect of V2O5 on the catalytic activity of Pt-based diesel oxidation catalyst. Applied Catalysis B: Environmental, 2003, 45, 269-279.	20.2	12
175	Effect of Preparation Method and Redox Treatment on the Reducibility and Structure of Supported Ceria–Zirconia Mixed Oxide. Journal of Catalysis, 2002, 209, 417-426.	6.2	162
176	Synergistic effect of vanadium and zirconium oxides in the Pd-only three-way catalysts synthesized by sol–gel method. Applied Catalysis A: General, 2001, 207, 69-77.	4.3	17
177	Effect of pH in a sol–gel synthesis on the physicochemical properties of Pd–alumina three-way catalyst. Applied Catalysis B: Environmental, 2000, 26, 285-289.	20.2	31
178	Title is missing!. Catalysis Letters, 2000, 70, 35-41.	2.6	49
179	Characteristics of the Pd-only three-way catalysts prepared by sol–gel method. Catalysis Today, 1999, 53, 575-582.	4.4	34
180	The effect of the preparation conditions of Pt/ZSM-5 upon its activity and selectivity for the reduction of nitric oxide. Applied Catalysis B: Environmental, 1999, 21, 183-190.	20.2	19

#	Article	IF	CITATIONS
181	Role of oxygen on NOx SCR catalyzed over Cu/ZSM-5 studied by FTIR, TPD, XPS and micropulse reaction. Catalysis Today, 1998, 44, 47-55.	4.4	22
182	In-situ IR studies of surface species during the selective catalytic reduction (SCR) of NO by propene over Cu-ZSM-5 zeolites. Studies in Surface Science and Catalysis, 1997, 105, 1557-1563.	1.5	4
183	Aromatization of pentane catalyzed over various metallosilicates. Korean Journal of Chemical Engineering, 1997, 14, 249-256.	2.7	8
184	The existence of dual Cu site involved in the selective catalytic reduction of NO with propene on Cu/ZSM-5. Catalysis Letters, 1996, 42, 177-184.	2.6	22
185	Controlling Multiple Active Sites on Pdâ^'CeO 2 for Sequential Câ^'C Cross oupling and Alcohol Oxidation in One Reaction System. ChemCatChem, 0, , .	3.7	1